

# 3D-Interaction Techniques for Planning of Oncologic Soft Tissue Operations

Bernhard Preim<sup>1</sup>, Wolf Spindler<sup>1</sup>, Karl J. Oldhafer<sup>2</sup>, Heinz-Otto Peitgen<sup>1</sup>

<sup>1</sup>MeVis – Center for Medical Diagnostic Systems and Visualization, Universitätsallee 29, 28359 Bremen, Germany  
Email: preim@mevis.de

<sup>2</sup>University Hospital Essen, Department for General and Transplantation Surgery

**Abstract.** We discuss interaction tasks and interaction techniques for the planning of soft tissue operations as for example oncologic liver and lung surgery. We focus on techniques to explore the relevant structures, to integrate measurements directly in 3d visualizations and to specify resection volumes. The main contribution of this paper is the introduction of new techniques for 3d measurements and for virtual resections. For both interaction tasks, dedicated widgets have been developed for the direct-manipulative use. In contrast to surgical simulators, which are used for the education of future surgeons, we concentrate on surgeons in the clinical routine and attempt to provide them with preoperative decision-support on the basis of patient-individual data.

The selection of the interaction tasks to be supported is based on a questionnaire in which 13 surgeons described their praxis of surgery planning and their requirements for computer support. All visualization and interaction techniques are integrated in a software, named SURGERYPLANNER, which exploits the results of image analysis achieved in an earlier project. With the SURGERYPLANNER the anatomical and pathological structures of individual patients are used for surgery planning.

**Keywords:** 3d interaction, visualization, medical graphics, computer-assisted surgery

## 1 Introduction

The treatment of malignant diseases targets at the complete destruction or removal of all tumors together with a sufficient safety free margin. At the same time life-critical anatomical structures must be saved. The appropriate therapy depends on tumor size, number and location in relation to anatomical structures.

In this paper, we focus on the planning of interventions to treat solid malignant tumors in organs, such as the liver, the lung, and the kidney. The anatomy of these organs is characterized by hierarchical vessel systems. Since vessel systems are tree-like structures, a

therapy which destroys a large blood vessel would at the same time interrupt the blood supply for a large part of the organ involved. In order to assess the risk of such a procedure, the volume of the organ which remains intact is a relevant measure. The main problem in the process of therapy planning<sup>1</sup> is the high variability in the shape and size of anatomical structures. Therefore, a clinically relevant visualization tool for surgery planning must be based on patient-individual data.

Currently, the treatment is planned with planar slices of CT- and MR-images. This leads to several problems: the spatial relationships between vessels and tumors are difficult to judge. The volume of tumors, the vessels involved in the therapy of a tumor and the region which is supplied by the involved vessels can only be estimated roughly.

In the following, we discuss interaction techniques to provide decision support for the above-mentioned questions. These are integrated in the SURGERY-PLANNER which contains three main components:

- a flexible 3d visualization for the exploration of the previously identified structures,
- an operation planning module which provides resection tools to explore a resection strategy (e.g. to simulate the removal of parts of an organ) and
- a measurement module which provides dedicated 3d widgets for the most crucial measurement tasks, such as distance measurements.

While the visualization component exploits well-known techniques, novel approaches are described for both virtual resection and for 3d-measurements. The SURGERY-PLANNER is intended to support preoperative decisions, to discuss an intervention and to explain it to a patient.

---

<sup>1</sup> The techniques described here are developed for surgery planning. Similar requirements exist, however, for minimally-invasive therapies, where tumors are destroyed for example by heat. Therefore, we use the more general term therapy planning.

## 2 Medical Background

A central issue of oncologic soft tissue operations is to take into account the individual vascular anatomy. As an example, we describe the vascular anatomy of the liver which is characterized by four hierarchical vessel systems: the portal venous system, the liver veins, the arteries and the bile ducts. For preoperative planning the portal venous system plays a key role because it defines the functional units of the liver – the *segments*. Hepatic veins drain the liver. According to the widespread Couinaud model [4] the liver consists of 8 segments which are defined as the regions supplied by a third order portal branch (third order refers to the bifurcation). Similarly, the lung anatomy is characterized by the bronchial tree and consists of 18 segments. Liver and lung segments are frequently used to discuss the location of a tumor. Unfortunately, segment boundaries either have no anatomical representation at all (in case of the liver) or they are not recognizable in clinical CT data (in case of the lung). Vessel systems enter an organ in the central part and bifurcate in their course to the periphery, where the vessel diameter reduces. Whether a tumor can be treated surgically often depends on the distance between the tumor and a major blood vessel.

In order to get a better understanding of the requirements, which surgeons actually have, we have polled surgeons by sending out some 30 questionnaires, from which 13 have been returned (all 13 are male, average age 42 years, experience in tumor surgery on the average 10 years). All surgeons indicated that the spatial relationships between vessels and tumors are difficult to judge and that a 3d visualization and quantitative analysis (e.g. distances and volumes) would be helpful for this purpose. Almost all, 12 of the 13 surgeons, indicated they would appreciate trying out resection strategies preoperatively which reveals that it is often not obvious, how to resect a tumor. In particular, if more than one tumor has to be treated, it is difficult to judge whether the tumors should be removed with a large cut, or with individual cuts for each tumor. The design of the SURGERYPLANNER and the focus on the specification of resection volumes as well as the integration of measurements are based on this survey.

## 3 Prior and Related Work

The work presented here is related to the field of surgery simulation. Surgery simulation is concerned with the modelling of surgical devices, the detection of collisions between surgical devices and tissue, the modelling of the elasticity of different tissue types, and finally with the simulation of deformations and cutting procedures. In [3] for example, deformations are simulated with finite elements which facilitate a precise

imitation of the realistic behavior at the expense of high computational costs. Mass-spring models, on the other hand allow near real-time interaction [11]. Recently, a framework for physically based modelling and cutting of soft tissue has been presented [1]. A sophisticated system for liver surgery simulation has been developed at INRIA [2, 7] which is based on the Visible Human dataset created by the National Institutes of Health. This work contributes to surgical education based on the interaction with virtual models.

In contrast to surgery simulation our focus is strictly guided by the requirements of (experienced) surgeons. We use the term *therapy planning* instead of *simulation* to emphasize the difference. For therapy planning, relevant questions include: Is a malignant disease curable? Which therapy is appropriate? Which volume must be resected? Which complications must be considered? To answer these questions, clinical data of the individual patient are required. This is the main difference in comparison to surgery simulation where often only one typical non-pathological dataset is employed.

Virtual resection and 3d-measurements are the major 3d interaction tasks we wish to support. To our knowledge, no related work exists which describes usability aspects for these interaction tasks. Current products for medical visualization either have no facilities to integrate 3d measurements or they use simple lines or polylines (to specify angles) for measurements. As lines are no true 3d objects, they are hard to select in 3d and it is very difficult to evaluate their placement in relation to anatomical structures.

Computer support for planning liver and lung resections is challenging. The identification and segmentation of the organs and of the tumors inside it, as well as the vessel segmentation, require excellent radiological data and a variety of dedicated methods which still form an area of active research.

The work presented here relies on image processing algorithms developed in our group in an earlier project. These include algorithms for organ and tumor segmentation, vessel segmentation, vessel analysis and segment approximation [12, 13]. Originally designed for the analysis of liver data sets, the algorithms have been refined to cope with CT lung images as well [5]. Vessel analysis comprises a skeletonization, the conversion to a graph which represents the branching hierarchy and the determination of segments (regions supplied by a subtree of the vascular structures).

While this paper is focussed on interactive therapy planning, an alternative approach would let the planning system “suggest” resection regions appropriate for the removal of tumors. We have described this approach and its limitations in [10].

## 4 Visualization for Therapy Planning

In the image processing stage, an organ, the tumors and the segments are identified in the original CT-data (100 .. 300 slices with 512×512 pixels per slice). For liver surgery planning the portal venous system and the hepatic veins are separated and the branches of the vessel system are detected. For lung surgery planning the bronchial tree is analyzed with similar methods. The voxel-object relationship is represented in a tagged volume (a volume with the same size as the data volume which contains an object-id per voxel).

### 4.1 Visualizing Anatomical and Pathological Structures

The SURGERYPLANNER uses the segmentation information to allow the user to design a 3d visualization. An OPENINVENTOR viewer with the usual features for camera control is used to explore the medical data. The viewer used in the SURGERYPLANNER extends the features of the ExaminerViewer in two ways: it provides a shadow projection on a camera-fix plane, and it supports 3d interaction with several 3d input devices. A library developed in-house with support for wire-frame, surface and volume visualization is used for rendering. For the exploration of the 3d visualization the following interaction tasks are supported:

- assign presentation variables to individual objects,
- filter objects (select the objects to be displayed),
- add annotations,
- add margin objects,
- compare different views of the data,
- assign transfer functions for volume rendering,
- adjust viewer parameters (e.g. shadow color).

For these tasks individual dialogs with carefully selected default values have been developed.

**Assign presentation variables.** Presentation variables include rendering styles, colors of vessel systems and segments, transparency values (for organs and segments to reveal structures inside). Default values for these variables, in particular colors, are derived by analyzing wide-spread text books (e.g. [8] and [9]). Fig. 1 presents a typical visualizations. To simplify the design of a visualization, objects are categorized (categories include vessels, tumors, segments, organs). Every adjustment of annotation styles or presentation variables can thus be applied to the whole category which makes it easier to generate consistent visualizations.

**Filter objects.** To avoid cluttered visualizations, facilities to filter objects are mandatory, because often about 50 relevant objects result from the image processing stage.

**Add annotations.** Annotations are used to integrate alphanumeric information from the image processing

stage. This includes the estimated volume of an object (often important for tumors) and the extent of the axis-aligned bounding box. The object name, and a note may also be included. Annotations are presented using 2d text which remains visible and legible after 3d transformations. As default, annotations are connected to the object to which they refer by lines and are placed at the border of the bounding box of the whole model. With this placement strategy text does not occlude the visualized objects.

**Add margin objects.** Surgical interventions target at the removal of pathological tumors with an additional margin (often 1 cm, sometimes up to 3 cm). For this purpose, the user can add margin objects for each selected visualization object. A margin is rendered transparently or as wire-frame to reveal what is inside (see Fig. 2, next page).

The comparison of views is discussed in Sect. 4.2.

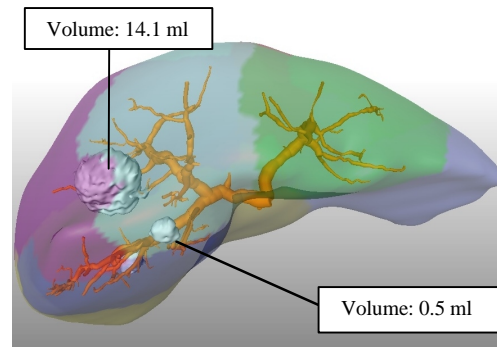


Fig. 1: Semitransparent liver segments with the portal venous system and three tumors rendered as surfaces. The visualization reveals the tumor-segment relationship and the vessels in the surrounding of each tumor. Annotations, like the tumor volume might be displayed at the periphery of the viewport.

### 4.2 Synchronization of Different Views

In the process of therapy planning a variety of visualizations is generated: the viewing direction is changed, different objects become visible, and resection tools (see Sect. 5) are applied. For many visualization goals no single visualization is appropriate. Therefore, it is crucial to allow the user to have multiple views which can be flexibly parametrized.

In each viewer all visualization parameters can be assigned independently. To support the comparison of different views (recall the interaction tasks specified in Sect. 4.1), the user can define synchronizations between selected viewers. Viewers may be synchronized for example concerning the application of resections, concerning filter operations and camera movements (Fig. 5). Moreover, in every dialog, which affects the content of a viewer, it can be specified whether these settings should be applied to all viewers (regardless whether synchronizations apply).

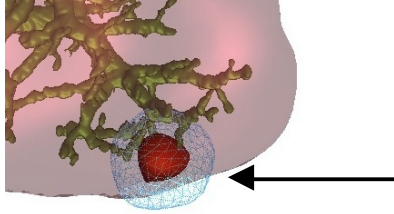


Fig. 2: Frontal view to the lower left part of the liver. A 1 cm safety margin around a tumor is defined and visualized with wire-frame. This allows to assess which vessels (portal venous system) would be affected by a resection of the tumor.

## 5 Specification of Resection Regions

Since surgeons want to try resection strategies, we developed techniques to remove arbitrary regions from a volume. Hierarchical data structures are employed to efficiently determine voxels involved in a resection. The algorithm can be used in a high-quality mode for real-time response and an accurate mode (described in [10]). In order to define a region which should be resected, (at least) two different approaches are possible:

- to define polygons or parametric curves which are moved along a straight line (extrusions) to define a volume. The interaction in this case is a punching process.
- to use tools as 3d erasers which delete all voxels which are touched by the movement of an eraser.

These different approaches are discussed in Sect. 5.1 and 5.2. For the usability of each strategy it is important that the user can evaluate the shape and size of the resection volume and can assess its location relative to anatomical structures.

### 5.1 Specification of Resections via Extrusions

Extrusions are widely used in geometric modelling systems to define 3d objects. Extrusions allow the user to specify regions of a regular shape (e.g. a prism as a simple example) with very little interaction. However, resection volumes are often not bounded by planar faces, but instead are irregularly shaped since the course of vessels and the shape of tumors are considered. The combination of extrusions to define a resection volume, such as a liver segment (recall Fig. 1), is tedious and counter-intuitive. Therefore, an extrusion may be suitable as an initial resection volume, but should be fine-tuned with eraser tools. In the SURGERY-PLANNER, a simple mechanism is realized which facilitates the extrusion of polygons, where the user can specify the depth range involved.

### 5.2 Specification of Resections with 3d Erasers

The use of erasers has complementary advantages and disadvantages compared to the use of extrusions: arbi-

trarily shaped regions can be specified more naturally and more precisely, however, with considerably more interaction effort. Two aspects are crucial for this type of interaction:

- The rasterization of a 3d eraser and its trace in the mask volume (recall [10]) must be fast enough to allow real-time interaction.
- The shape and size of 3d erasers must be flexible in order to facilitate a coarse as well as a detailed specification of the resection volume.

Two general approaches are feasible for the use of 3d erasers. The first is strictly adhered to the direct-manipulative interaction style: the eraser is visualized explicitly and moved by an appropriate 3d widget with handles for 6 degree of freedom-translation. We will refer to this approach as *explicit resection*. A conventional 2d input device as well as a 3d input device may be employed for this interaction. The second approach is less direct: the eraser can be translated by moving a 2d mouse and holding a mouse button pressed. Neither the 3d eraser nor handles are visible. This approach, which we call *no-widget-resection*, is motivated by the desire to have an unoccluded view to the visualization.

#### 5.2.1 Explicit Resection

We developed different 3d erasers: wedges, cylinders and spheres. The shape of the 3d erasers is restricted to be convex, however arbitrary resection shapes can be constructed with them. Wedges are inspired by wedge-resections – a typical resection form in liver and lung surgery. Erasers can be parameterized within appropriate dialogs and can be transformed in a 3d visualization by means of manipulators provided by the Graphics Library OPENINVENTOR (see Fig. 3). The properties of an eraser define its visualization (color, rendering style) and its initial orientation and position.

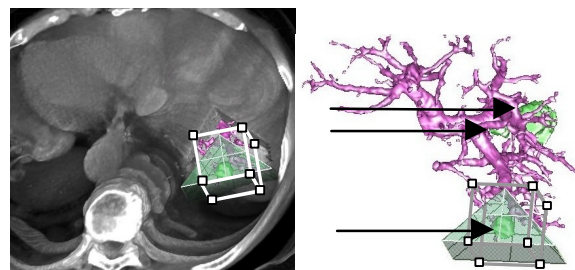


Fig. 3: A wedge-shaped eraser is used for virtual resection in a CT data set. The user can resect in either view. In the left view the user gets an impression of the resection, while the right view is used for the planning (as all tumors are visible, see the arrows). The manipulators are redrawn for better recognizability.

3d erasers and their manipulators should be recognizable but should not occlude the resection region

heavily. As a trade-off semitransparent erasers and erasers which are visualized via their outlines are used. Manipulators provide support for all transformation tasks: translation, rotation and scaling. After the size has been adjusted, an eraser is primarily translated and less often rotated. Based on this observation 3d erasers should be equipped with a manipulator dedicated for translation. The OPENINVENTOR Jack-Manipulator is appropriate for this task. With this manipulator, translations in the orthogonal planes are explicitly supported. The Jack-Manipulator can also be used to rotate an object. For this purpose a second mode exists with handles for translations temporarily hidden.

### 5.2.2 No-Widget-Resection

To avoid the occlusion of the scene with an eraser and the associated manipulator, the *no-widget-resection* was realized. In this approach, only a cross-hair symbol represents the current cursor position. The shape, size and orientation of the eraser can be chosen in the same manner as described in Sect. 5.2.1. In the virtual model that part of the scene is marked as deleted which corresponds to the selected eraser parameters. If the cursor is moved to a position (in 2d screen coordinates), where it has not been before, the nearest part of the scene is deleted. If the cursor arrives again at such a position, a deeper part of the volume is deleted (the  $z$ -coordinate is increased by the size of the underlying eraser). The interaction becomes faster (and more predictable) if the effect of the virtual resection can be restricted to a range of transparency values. Thus, a transfer function<sup>2</sup> may be adjusted in such a way that structures of little importance for therapy planning are displayed strongly transparent. Based on such a transfer function the virtual resection might be applied only to those voxels with transparency values above an appropriate threshold. Thus, little time is wasted to virtually resect structures, which are not relevant for the therapy (and would not be destroyed in the real therapy).

### 5.2.3 Comparison of Virtual Resection Techniques

The *no-widget-approach* is less intuitive since neither a widget nor handles for its movement are displayed. In the explicit resection-approach the user has more feedback, as the eraser's movement can be watched. Therefore, real-time demands are of higher importance for the no-widget-approach.

The explicit resection approach can benefit from 3d input devices and facilitates direct-manipulative scaling and rotation of the eraser whereas in the no-widget-approach the eraser can only be translated. As transla-

<sup>2</sup>A transfer function defines the mapping of intensity values of the original data to grey and opacity values.

tions are the dominant transformation in virtual resections this is less important.

Despite these disadvantages, informal tests indicated that the no-widget-approach is the superior solution, because the interaction is more efficient. As the visualization is not occluded, the results of the virtual resection can be better evaluated. Moreover, every movement of the cursor really changes the resection volume. By contrast, in the explicit resection approach the user may delete the same region again and again until she becomes aware that the eraser must be translated.

### 5.3 Selective Resection

Resection volumes can be applied selectively to different structures so that certain objects are visible, even if they belong to the resection region. Such visualizations have been used for anatomy education [15]. For therapy planning it is extremely valuable to see a tumor and major blood vessels in a region where a resection is intended. The user can thus assess the distance between the tumor and the boundary of the resection region as well as the vessels involved in this resection.

### 5.4 Use of Resection Tools

The typical use of 3d erasers proceeds in the following way: the user starts with a medium-sized eraser and moves it to remove a tumor. In this process, it is often necessary to rotate the whole model to evaluate what has been removed. After a rough boundary has been specified it is refined with a smaller-sized 3d eraser. Gaps in the resection region may be ignored as these may be filled automatically in a post-process. As the resection volume is explicitly represented, 3d image-processing techniques, like dilation and erosion can be applied to extend/shrink the resection volume globally.



Fig. 4: The resection specified in the right 3d visualization with the no-widget-approach is also marked in the slice view on the left 2d viewer as blue region. The crosses indicate the current position in either view.

For the use of explicit 3d erasers a two-handed interaction with the system is possible, with one hand controlling the resection (with a 3d input device), and the other to simultaneously control the camera (with a 2d mouse). Independent of the method chosen for the virtual resection, it can be better controlled if manipu-

lations are applied to two views simultaneously which display the virtual model from different viewing angles. These views should be synchronized appropriately (recall Sect. 4.2). Another important aspect for the usability of virtual resections is the feature that the resection volume can be assessed in combination with planar views of the original data. We developed this feature so that the user can step through the original data where the resection region is transparently overlaid and marked with a different color (see Fig. 4). This is crucial, as surgeons are accustomed to discuss resections by drawing in (copies of) the original 2d data.

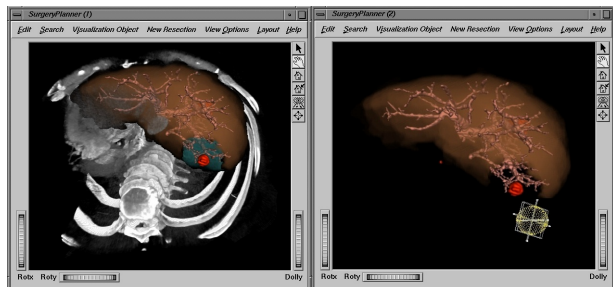


Fig. 5: Two synchronized views for the specification of a resection. The left view contains the bones and other structures as anatomical context, while the right view contains only the intrahepatic structures and is used to plan the movement of the resection tool. In the left view direct volume rendering and surface-based rendering are overlaid.

## 6 Measurements in 3d Visualizations

Currently, it is common practice in radiological workstations to use 2d measurement tools to define distances, diameters, or angles in planar slices of radiological data. This, however, gives only a rough estimation for questions such as the minimal distance between two 3d objects. Therefore, 3d measurement tools are required to integrate measurements in 3d visualizations. The development of 3d measurement tools to be used in the context of a complex 3d visualization is difficult because the user has to be provided with enough depth cues to assess the position and orientation of such a measurement tool (otherwise the precision pretended by exact numbers is misleading). A “simple” transition of line-based 2d measurement tools into 3d is not sufficient for this purpose.

The interactive use of measurement tools is flexible, however, it requires a certain effort on the user’s part. Therefore, we carefully analysed which interaction tasks are of primary importance in order to support these tasks by an automatic approach. These tasks include the definition of the extent of objects as well as distance measurements. Of paramount importance for the risk analysis is the minimal distance between pathological structures and risk structures. For the following,

we assume that the segmentation information has been converted into a boundary representation. The measurement tool described in this section are part of a library of 3d measurement tools, which also comprises 3d widgets for angle and area measurements.

### 6.1 Interactive Distance Measurement

An interactive *distance line* widget for distance measurements consists of a small cone (3d representation of arrowheads) and a small cylinder (3d representation of the line). With this design the distance line is a recognizable 3d object. As an additional orientation aid distance lines may cast a shadow. The placement of the number is adapted to the line length: if the line is long enough the cylinder is interrupted for the placement of the number in the center (see Fig. 6). Otherwise the number is placed near one of the endpoints of the distance line. The distance line as a whole as well as individual endpoints can be translated by an appropriate dragger. The distance line is created with rubberbanding, and the distance number is updated continuously. To ease the translation of the measurement instrument, snapping is included. With this feature the endpoint translated by the user is attracted by the surface of an object. Snapping is motivated by the fact that the most common measurement tasks include the determination of the distance between object surfaces.

The calibration of distance measurement facilities is based on the header information of radiological data which includes the size of a voxel (for example  $0.7 \times 0.7 \times 2$  mm with the larger value representing the distance between slices).

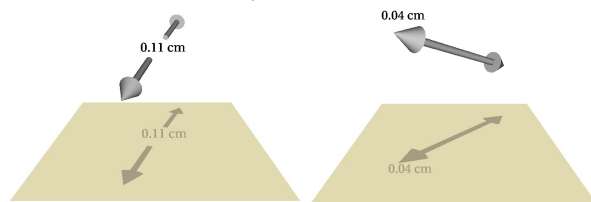


Fig. 6: Distance lines with their shadow projections. The placement of the number depends on the available space. The accuracy of the measurement is determined by the voxel size of the underlying data.

### 6.2 Definition of the Object Extent

For preoperative planning the extent of pathological structures is important. It is used to define the stage of a malignant disease which is relevant for any therapy decision. The extent of a tumor is defined as the longest side of the oriented bounding box (OBB). The OBB of object  $o$  is defined by a principal component analysis. For this purpose the center of gravity (COG) of  $o$  is calculated, the covariance matrix  $A$  (a symmetric  $3 \times 3$ -matrix) is calculated taking into account all vertices of

$o$ . The normalized eigenvectors of  $A$  form a local right-angled coordinate system with origin at the center of gravity. The normalized eigenvectors of  $A$  form a rotation matrix, which is known as the Jacobian matrix  $C$ . This process is referred to as principal component analysis [14]. In order to get the exact extent in each of the 3 directions,  $o$  is transformed to  $o'$  by rotating  $o$  according to  $C$ . As  $o'$  is axis-aligned, the axis-aligned bounding box (ABB) of  $o'$  can be easily determined. The length of the axes of the ABB represent the length of the main axis. The extent is visualized by three orthogonal distance lines (see Sect. 6.1) with the same length as the OBB and the intersection at the COG. This process is illustrated in Fig. 7. Numbers are placed at the endpoints in order to reduce the problem of overlapping numbers. As the distance lines proceed inside, the object for which these measurements have been performed is rendered semitransparently (see Fig. 8).

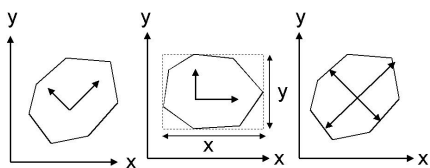


Fig. 7: Eigenvectors of an object are defined using the covariance matrix (left). Object  $o$  is rotated according to the Jacobian-Matrix to define the oriented bounding box (middle). Object  $o$  is rotated back and the main axis is visualized with distance lines (right).

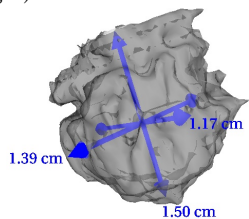


Fig. 8: The extent of a tumor is determined by defining the oriented bounding box (OBB). The extent is visualized by three orthogonal distance lines.

### 6.3 Definition of Minimal Distances

Minimal distances between the structures which need to be treated and structures at risk are crucial for therapy planning. Therefore, we make it possible to define automatically the minimal distance between two selected objects. The minimal distance between two polyhedra  $A$  and  $B$  might occur at faces, edges or vertices. Here, we simplify the task by considering only vertices and searching for the vertices  $a_{min}$  and  $b_{min}$  with minimal distance. This simplification introduces an error which can be neglected for objects in medical data as they consist of thousands of vertices resulting from equal sampling.

The brute-force method for this purpose is to calculate the distance between all vertices  $a_i$  of object  $A$  and  $b_j$  of object  $B$ , and then to minimize. This simple

approach is too slow, if objects with many vertices occur. Methods for the efficient determination of minimal distances have been developed for collision detection in dynamic scenes (e.g. [6]). These algorithms employ hierarchical data structures (decomposition of the scene) and hierarchies of enclosed objects to quickly reduce the number of vertices to be considered. The construction of these hierarchical data structures, however, takes considerable time which is acceptable for dynamic scenes (where the distance calculation is often repeated). For the calculation of distances between objects in static models of the patient anatomy the additional effort is not justified.

We briefly sketch an algorithm which is based on the observation that the minimal distance between the polyhedra  $A$  and  $B$  is smaller or equal than the distance between the centers of gravity  $COG_A$  and  $COG_B$ . After  $COG_A$  and  $COG_B$  are determined the distance between  $COG_B$  and  $a_i$  is calculated (for each  $a_i$ ). Each  $a_i$  with

$$dist(a_i, COG_B) > dist(COG_A, COG_B)$$

is not considered in the further procedure.<sup>3</sup> Similarly, the distance between  $COG(A)$  and  $b_j$  is calculated. All  $b_j$  with

$$dist(b_j, COG_A) > dist(COG_A, COG_B)$$

are excluded from the further process.

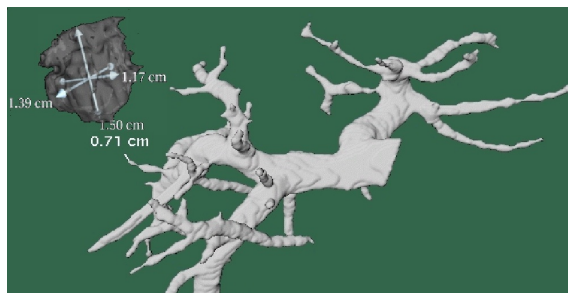


Fig. 9: The minimal distance between a vessel system (portal vein in the liver) and a tumor is automatically determined.

After one step the number of vertices to consider is on average approximately reduced to one half. The procedure is repeated by calculating COGs for the reduced sets of vertices. This process is finished if the number of points to consider is below a given threshold. For the remaining vertices, the brute-force approach of minimization of all possible distances is applied. The algorithm works well, except for objects, where the convex hulls overlap. In this case the algorithm cannot be applied. The minimal distance between two objects is visualized by a distance line (recall Sect. 6.1) starting at the vertex  $a_{min}$  and ending by  $b_{min}$  (see Fig. 9). The measurement task could be further supported: for all objects within a certain diameter around a tumor (e.g. 3 cm) the minimal distance is calculated and visualized.

<sup>3</sup>  $dist(a,b)$  represents the Euclidean distance.

## 6.4 Use of Measurement Tools

3d widgets for measurements in 3d visualizations are manipulated using compositions of OPENINVENTOR draggers. Measurement tools are automatically named (the name is derived from the type and a sequential number of the tool) and can be selectively displayed and hidden. All measurement tools use 2d text for the numbers. Thus the numbers remain legible after rotations occur. A measurement is stored together with the viewing direction at the time of its specification. Later, the measurement might be selected in a list, and as a consequence, this original viewing direction is used.

For oncologic soft tissue operations distance measurements are of highest importance. Angle measurements are more essential for orthopaedic interventions. An angle measurement widget has been developed for this purpose. By using additional planes (orthogonal to the sides of the angle) the user can modify an angle like opening or closing a book. To avoid that the visualization is cluttered, these planes are rendered semitransparently. The orientation aids are inspired by manipulators of the OPENINVENTOR-library.

## 7 Conclusion and Future Work

We presented new interaction techniques for virtual resection and 3d distance measurements using dedicated 3d widgets. The resection tools follow two paradigms, extruded shapes and interactive “erasers”. While interactive response is maintained through limiting the erasers to a convex shape, arbitrary resections are possible through “eraser” traces. Tools for the interactive and automatic measurement of 3d objects have been presented with focus on their application for therapy planning. These new techniques have been integrated with known techniques for the visualization of medical volume data in the SURGERYPLANNER. This system provides a reliable base to aid in the complex decision making process regarding the operability of patients with solid tumors inside the liver and lung. The system has been informally tested with focus on the visualization and resection tools. The selective application of resection tools and synchronization mechanisms are essential for the usefulness of the system.

In practice, it is intended such that a radiologist operates the system and a surgeon tells her what she likes to see. In this way interventions are planned today: radiologists – specialized in the use of dedicated workstations – demonstrate surgeons clinical data in the desired way. An in-depth evaluation of the SURGERYPLANNER is underway. The system has been introduced in two university hospitals to answer questions like which kinds of interaction techniques are used frequently, how precise are interactive 3d measurements, and

how does the preoperative planning influence the decisions taken by a surgeon.

## Acknowledgements

We want to thank our clinical partners for fruitful discussions and for providing us with excellent radiological data (Prof. Galanski, Med. School Hannover) and Prof. Klose (University hospital Marburg). Furthermore, we thank our colleagues A. Schenk, Dr. D. Selle and Dr. S. Krass for the development of the image-processing. H. Sonnet, University of Magdeburg implemented the measurement tools. Many thanks go to the reviewers for their comments. We also acknowledge the support of the German Research Council (Grant No. 199/9-1).

## References

- [1] Bielsen D, Maiwald VA and Gross MH (1999) „Interactive Cuts through 3-Dimensional Soft Tissue“, *Proc. of Eurographics'99*, pp. 31-38
- [2] Boux de Casson F and Laugier C (1999) “Modeling the Dynamics of a Human Liver for a Minimally Invasive Surgery Simulator”, *Proc. of Medical Image Computing and Computer-Assisted Intervention*, Springer, LNCS, Vol 1679, pp. 1156-1165
- [3] Bro-Nielsen, M and Cotin S (1996) „Real-time volumetric deformable models for surgery simulation using finite elements and condensation“, *Proc. of Eurographics'99*, pp. 57-66
- [4] Couinaud, C. *Le foie – Etudes anatomiques et chirurgicales*, Paris, Masson, 1957
- [5] Krass, S, Selle D, Böhm D et al. (2000) “A method for the determination of bronchopulmonary segments from HRCT data” *Proc. of Computer-Assisted Radiology and Surgery (CARS 2000)*, Elsevier, pp. 584-589
- [6] Lennerz, C, Schömer E and Warken T (1999) „A Framework for Collision Detection and Response“, *Proc. of 11<sup>th</sup> European Simulation Symposium, ESS'99*, pp. 309-314
- [7] Marescaux J, Clement JM, Tasseti V et al. (1998) “Virtual reality applied to Hepatic Surgery Simulation: The Next Revolution”, *Annals of Surgery*, Vol 228 (5), pp. 627-634
- [8] Mazziotti A and Cavallari A (1997) *Techniques in Liver Surgery*, Greenwich Medical Media
- [9] Netter, FH (1995) *Atlas of Human Anatomy*, 8<sup>th</sup> edition, Ciba Geigy Corporation, Summit New Jersey
- [10] Preim, B, Selle, D, Spindler, W, Oldhafer KJ and Peitgen HO (2000) “Interaction Techniques and Vessel Analysis for Preoperative Planning in Liver Surgery”, *Proc. of Medical Image Computing and Computer-Assisted Intervention*, Springer, LNCS, Vol. 1935, pp. 608-617
- [11] Radetzky A, Nürnberger A and Pretschner DP (2000) “Elastodynamic Shape Modeller: A Tool for Defining the Deformation Behavior of Virtual Tissues”, *Radiographics*, Vol. 20 (3), pp. 865-881
- [12] Schenk A, Prause G and Peitgen HO (2000) “Efficient Semi-Automatic Segmentation of 3D Objects in Medical Images”, *Proc. of MICCA*, Springer, LNCS, Vol. 1935, pp. 186-195
- [13] Selle D, Schindewolf T, Evertsz CJG and Peitgen HO (1999) “Quantitative analysis of CT liver images”, *Excerpta Medical International Congress*, Vol 1182, Elsevier, pp. 435-444
- [14] Sonka M, Hlavac V, Boyle R (1999) *Image Processing, Analysis and Machine Vision*, Brooks-Coyle, Second Edition
- [15] Tiede U, Bomans M, Höhne KH et al. (1993) “A computerized three-dimensional atlas of the human skull and brain”, *Am. J. Neuroradiology*, Vol 14 (3), pp. 551-559